1296 *Biochemistry* **2011,** *50,* 1296–1308
DOI: 10.1021/bi1013613

BIOCHEMISTRY
including biophysical chemistry & molecular biology
Article

Distinct Ligand Specificity of the Tiam1 and Tiam2 PDZ Domains[†]

Tyson R. Shepherd,[‡,⊥] Ryan L. Hard,[⊥,∥] Ann M. Murray,[‡] Dehua Pei,[∥] and Ernesto J. Fuentes*[,‡,§]

[‡]*Department of Biochemistry, Roy J. and Lucille A. Carver College of Medicine, and* [§]*Holden Comprehensive Cancer Center, University of Iowa, Iowa City, Iowa 52242-1109, United States, and* [∥]*Department of Chemistry and Ohio State Biochemistry Program, The Ohio State University, Columbus, Ohio 43210, United States.* [⊥]*These authors contributed equally to this work.*

Received August 23, 2010; Revised Manuscript Received December 8, 2010

ABSTRACT: Guanine nucleotide exchange factor proteins of the Tiam family are activators of the Rho GTPase Rac1 and critical for cell morphology, adhesion, migration, and polarity. These proteins are modular and contain a variety of interaction domains, including a single post-synaptic density-95/discs large/zonula occludens-1 (PDZ) domain. Previous studies suggest that the specificities of the Tiam1 and Tiam2 PDZ domains are distinct. Here, we sought to conclusively define these specificities and determine their molecular origin. Using a combinatorial peptide library, we identified a consensus binding sequence for each PDZ domain. Analysis of these consensus sequences and binding assays with peptides derived from native proteins indicated that these two PDZ domains have overlapping but distinct specificities. We also identified residues in two regions (S_0 and S_{-2} pockets) of the Tiam1 PDZ domain that are important determinants of ligand specificity. Site-directed mutagenesis of four nonconserved residues in these two regions along with peptide binding analyses confirmed that these residues are crucial for ligand affinity and specificity. Furthermore, double mutant cycle analysis of each region revealed energetic couplings that were dependent on the ligand being investigated. Remarkably, a Tiam1 PDZ domain quadruple mutant had the same specificity as the Tiam2 PDZ domain. Finally, analysis of Tiam family PDZ domain sequences indicated that the PDZ domains segregate into four distinct families based on the residues studied here. Collectively, our data suggest that Tiam family proteins have highly evolved PDZ domain−ligand interfaces with distinct specificities and that they have disparate PDZ domain-dependent biological functions.

The T-cell lymphoma invasion and metastasis 1 (Tiam1) protein and its homologue, Tiam2, also known as STEF (SIF- and Tiam1-like exchange factor), are guanine nucleotide exchange factor proteins that specifically activate the Rho family GTPase Rac1 (*1*, *2*). Tiam1 is important for the integrity of adherens junctions (*3*, *4*), tight junctions (*5*, *6*), and cell−matrix interactions (*7*, *8*). In addition, Tiam1 is involved in axon formation (*9*) and neurite outgrowth (*10*−*13*). Deregulation of Tiam1 has been implicated in invasive and metastatic forms of lung (*14*) and colorectal (*15*) cancer and may be a predictor of poor patient outcome for renal cell (*16*), prostate (*17*), and hepatocellular (*18*) carcinomas. Tiam2 has been shown to be important for focal adhesion disassembly (*19*), neuronal development, and neurite growth (*20*, *21*), yet its role in disease has not been established. In mammalian cells, the spatial and temporal regulation of Tiam-like proteins is achieved via distinct protein−protein interaction domains. However, the mechanisms that regulate each of these interaction domains are not fully understood.

Tiam1 and Tiam2 are both composed of a set of diverse interaction domains, including a Pleckstrin homology-coiled-coil-extension (PH_n-CC-Ex) cassette that is important for subcellular localization, a Ras binding domain (RBD) known to bind activated Ras, a Dbl homology-Pleckstrin homology ($DH\text{-}PH_c$) catalytic bidomain that activates Rac1, and a post-synaptic density-95/discs large/zonula occludens-1 (PDZ)[1] domain that binds cell adhesion molecules (Figure 1A). PDZ domains are ubiquitous protein−protein binding domains found in bacteria and eukaryotes (*22*, *23*) that typically interact with carboxy-terminal residues 4−10 of partner proteins to form higher-order signal transduction complexes. Recent studies identified Syndecan1 (*8*) and CADM1 (*24*) as PDZ domain-binding proteins for the Tiam1 PDZ domain, but to date, no binding partners have been reported for the Tiam2 PDZ domain. Although other interaction domains have a high degree of sequence identity across the Tiam family of proteins, the Tiam1 and Tiam2 PDZ domains are only ∼28% identical (Figure 1A,B). This suggests potential differences in ligand specificity and biological function.

Previously, we determined the structure of the Tiam1 PDZ domain free and bound to a model peptide ligand (*8*). This structure shows that the peptide binding cleft is formed by β2 and α2 of the PDZ domain, and that ligand specificity is partially derived from two pockets (S_0 and S_{-2}, S for site) (Figure 1C,D). The S_0 pocket

[†]This work was supported by funds from the National Science Foundation (MCB-0624451 to E.J.F.), the American Heart Association (0835261N to E.J.F.), and the National Institutes of Health (NIH) (GM062820 to D.P.). T.R.S. was supported in part by an NIH predoctoral fellowship in Pharmacological Sciences (GM067795) and by a University of Iowa Graduate Student Fellowship sponsored by the Center for Biocatalysis and Bioprocessing. R.L.H. was supported by a predoctoral fellowship from the NIH Chemistry-Biology Interface Training Program (GM08512).

*To whom correspondence should be addressed. Telephone: (319) 353-4244. Fax: (319) 335-9570. E-mail: ernesto-fuentes@uiowa.edu.

[1]Abbreviations: GEF, guanine nucleotide exchange factor; NMR, nuclear magnetic resonance; OBOC, one-bead-one-compound; PDZ, post-synaptic density-95/discs large/zonula occludens-1; PED−MS, partial Edman degradation mass spectrometry.

 Published on Web 12/30/2010

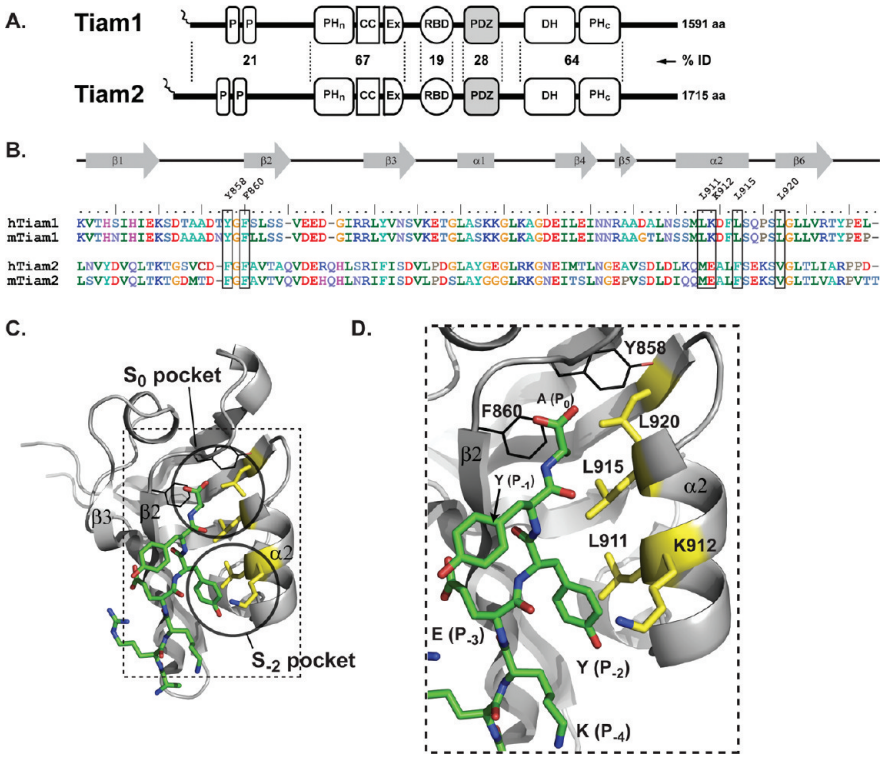

FIGURE 1: Conservation and structure of the Tiam1 and Tiam2 PDZ domains. (A) Domain architecture and motifs within Tiam family GEF proteins: DH, Dbl homology domain; PH, Pleckstrin homology domain; CC, coiled-coil domain; Ex, extension domain; RBD, Ras-binding domain; PDZ, PSD-95/Dlg/ZO-1 domain; and P, PEST sequence. Myristoylation is indicated by the twisting line at the N-terminus. The percent identity (% ID) between each homologous domain is indicated. (B) Amino acid residues involved in Tiam1 and Tiam2 PDZ domain specificity. Primary sequence alignment of Tiam1 and Tiam2 PDZ domains with residues that are discussed in the text labeled and boxed. (C) Ribbon diagram of the Tiam1 PDZ domain−Model peptide complex (Protein Data Bank entry 3KZE) (*8*). (D) Expanded view of the boxed region in panel C showing the residues targeted for mutagenesis (colored yellow) in this study.

is formed by the side chains of F860, Y858, L915, and L920 and accommodates the side chain of the most C-terminal residue of the ligand (P_0, where P_{-n} denotes the residue position n amino acids from the C-terminus). Residues L911 and K912 form the S_{-2} pocket that accommodates the side chain of the ligand at P_{-2}. NMR-based titrations of the Tiam1 PDZ domain with C-terminal eight-residue peptides that differ primarily at position P_0 (Syndecan1 and Caspr4) showed that the chemical shifts of L911, K912, and L915 were significantly perturbed upon binding of the Syndecan1 peptide, but not upon binding of the Caspr4 peptide. In contrast, the chemical shift of L920 was not perturbed upon binding of Syndecan1 but was shifted upon binding of the Caspr4 peptide (*8*). These data suggest that residues L911, K912, L915, and L920 are determinants for Tiam1 PDZ domain specificity. Notably, these residues are not conserved between the Tiam1 and Tiam2 PDZ domains (Figure 1B), further suggesting that there might be differences in Tiam1 and Tiam2 PDZ domain specificity.

The specificity of the Tiam1 and Tiam2 PDZ domains for C-terminal ligands has been previously investigated, but the results from these studies appear to be inconsistent. Songyang et al. (*25*) used immobilized PDZ domains to select binding peptides derived from a synthetic, randomized peptide library and determined that the Tiam1 PDZ domain had a preference for ligands with Ala and Phe at position P_0 (*25*). Using phage display, Tonikian et al. (*26*) determined the specificity for approximately half of the PDZ domains found in humans, including the Tiam1 and Tiam2 PDZ domains. The consensus sequence determined by Tonikian et al. (*26*) for the Tiam1 PDZ domain was in reasonable agreement with that found by Songyang et al. (*25*). For the Tiam2 PDZ domain, however, there is an apparent inconsistency among the reported specificities. Tonikian et al. (*26*) reported a clear preference for Val at position P_0, whereas Stiffler et al. (*27*) identified Caspr4, which contains a C-terminal Phe, as a Tiam2 PDZ domain-binding protein using a fluorescence-based protein microarray assay. These discrepancies prompted us to conduct a comprehensive study comparing the specificity of the Tiam1 and Tiam2 PDZ domains. We screened a combinatorial peptide library to determine the consensus binding sequence for each PDZ domain and found they possess overlapping but distinct specificities. These differences were corroborated by binding assays using several physiologically relevant ligands and resolve the apparent inconsistency regarding the specificity of the Tiam2 PDZ domain. Furthermore, we identified four residues in the Tiam1 PDZ domain that are crucial for the differences in specificity and investigated their thermodynamic origin by site-directed mutagenesis and double-mutant cycle analyses. Finally, mutation of these four residues in the Tiam1 PDZ domain was sufficient to switch its specificity to that of the Tiam2 PDZ domain.

MATERIALS AND METHODS

Protein Expression and Purification. The Tiam1 PDZ domain expression plasmid has been described previously (*8*). All Tiam1 PDZ domain mutants (single, double, and quadruple) were produced using oligonucleotide-directed mutagenesis (QuikChange, Stratagene) with the wild-type or mutant Tiam1 PDZ domain DNA as a template. All mutants were verified by automated DNA sequencing (University of Iowa DNA Facility). The Tiam2 PDZ domain expression plasmid was constructed by

amplification of the DNA sequence encoding the PDZ domain (residues 809−994) from the full-length mouse Tiam2 sequence using polymerase chain reaction (PCR) (*28*). The amplified PDZ domain DNA was ligated into a modified pET21a vector (Novagen) that contains an N-terminal His_6 tag and a tobacco etch virus (rTEV) protease cleavage site. The nucleotide coding sequence of the pET21a-Tiam2 PDZ vector was verified by automated DNA sequencing (University of Iowa DNA Facility). Glutathione *S*-transferase (GST)-fused Tiam1 and Tiam2 PDZ domains were constructed by subcloning the PDZ domain-encoding DNA into a modified pGEX vector (GE Healthcare).

All proteins were produced in BL21(DE3) (Invitrogen) *Escherichia coli* cells. Typically, *E. coli* cells were grown at 37 °C in Luria-Bertani (LB) medium supplemented with ampicillin (100 μg/mL) under vigorous agitation until an A_{600} of 0.6−1.0 had been reached. Cultures were subsequently cooled to 25 °C, and protein expression was induced by the addition of isopropyl 1-thio-D-galactopyranoside to a final concentration of 1 mM. Induced cells were incubated for an additional 6−8 h at 25 °C and harvested by centrifugation.

The histidine-tagged Tiam1 and Tiam2 PDZ domains were purified by nickel-chelate and size-exclusion (G-50 or S-75) chromatography (GE Healthcare). The N-terminal His_6 affinity tag was removed by proteolysis by incubation of the histidine-tagged PDZ protein with recombinant rTEV protease for 12−16 h at room temperature. Undigested fusion protein, cleaved His_6 tag, and histidine-tagged rTEV were separated from the digested PDZ domain by nickel-chelate chromatography. The final yield was ~20 mg of PDZ protein from 1 L of culture, at ~95% purity as judged by sodium dodecyl sulfate−polyacrylamide gel electrophoresis. Samples were used immediately or stored at −20 °C. GST−Tiam1 and GST−Tiam2 PDZ domain fusion proteins were purified by standard affinity chromatography using glutathione Sepharose 4B medium (GE Healthcare) followed by size-exclusion (S-75) chromatography. The concentration of the protein in solution was determined by measuring the UV absorbance at 280 nm using the extinction coefficient of the protein calculated from the protein sequence (SEDNTERP version 1.09).

PDZ Domain Labeling for Combinatorial Library Screening. GST−Tiam1 and GST−Tiam2 PDZ domain proteins (≥2 mg/mL) were labeled with biotin by incubation with 2 equiv of (+)-biotin *N*-hydroxysuccinimide ester (Sigma) in 0.1 M $NaHCO_3$ (pH 8.4) for 30 min. The reaction was quenched by the addition of 50 μL of 1 M Tris buffer (pH 8.4). The reaction mixture was passed through a G-25 size-exclusion column (eluted with phosphate-buffered saline) to remove any free biotin. The proteins were also labeled with Texas Red (Texas Red-X succinimidyl ester, Invitrogen) in a similar manner (2 equiv of Texas Red, 45 min reaction, and quenching with 5 μL of 1 M Tris buffer).

Library Screening against Biotinylated PDZ Domains. An inverted peptide library was synthesized on 2.0 g of TentaGel S NH_2 resin (90 μm, 0.29 mmol/g, 2.86×10^6 beads/g) and characterized as previously described (*29*). For a typical screening experiment, 10−50 mg of the library resin was swollen in dichloromethane (DCM) in a 1.2 mL spin column (Micro Bio-Spin, Bio-Rad) for 2 h, washed with dimethylformamide (DMF) and water, and suspended in HBST-gelatin buffer [30 mM HEPES, 150 mM NaCl, 0.05% Tween 20, and 0.1% gelatin (pH 7.4)] for 4 h. The resin was drained and resuspended in the HBST-gelatin buffer containing 1−2 μM biotinylated PDZ domain protein. After overnight incubation at 4 °C (with shaking), the protein solution was removed and the resin resuspended in streptavidin−alkaline phosphatase (SA-AP) buffer [10 mM $MgCl_2$, 30 mM Tris-HCl, 70 μM $ZnCl_2$, and 250 mM NaCl (pH 7.4)] with 1 μg/mL SA-AP buffer. After 10 min at 4 °C, the resin was drained and then washed twice with the SA-AP buffer and twice with SA-AP reaction buffer [5 mM $MgCl_2$, 30 mM Tris-HCl, 20 μM $ZnCl_2$, and 100 mM NaCl (pH 8.5)]. The resin was transferred into one well of a 12-well plate (BD Falcon) using SA-AP reaction buffer. After the addition of 100 μL of 5 mg/mL 5-bromo-4-chloro-3-indolyl phosphate (BCIP), the resin was incubated at room temperature on a rotary shaker until positive beads took on a turquoise color. The staining reaction was terminated by the addition of 100 μL of 1 M HCl to the resin, and the positive beads were removed manually with a micropipet with the aid of a dissecting microscope. The positive beads were individually sequenced by a partial Edman degradation−mass spectrometry (PED−MS) method (*30*).

Library Screening against Texas Red-Labeled PDZ Domains. Typically, 10−50 mg of the peptide library resin was swollen and washed in DCM, DMF, water, and the gelatin buffer as described previously (*29*). The resin was then transferred to a Petri dish (60 mm × 15 mm) (BD Falcon), and fluorescently labeled protein was added to produce a final concentration of 0.7−1 μM. The dishes were incubated overnight at 4 °C with gentle shaking. The resulting beads were then examined under an Olympus SZX12 fluorescence microscope (Texas Red filter), and beads having the brightest red fluorescence were isolated using a micropipet and sequenced by PED−MS (*30*).

Consensus Binding Motif and SMALI Matrix. For each PDZ domain, all of the peptide sequences selected from the library were initially sorted into different subgroups (I−IV) on the basis of sequence similarities using Microsoft Excel. Each subgroup of sequences was next analyzed by scoring matrix-assisted ligand identification (SMALI) to construct a position-weighted matrix for the protein domain (*31*). For each position in a peptide sequence, all 20 amino acids were assigned a score using Microsoft Excel and the formulas

$$R_{i,p} = X_{i,p} / \sum_{i=1}^{N} X_{i,p}$$

$$S_{i,p} = R_{i,p}[\log_2 N - \sum_{i=1}^{N} (R_{i,p} \log_2 R_{i,p})]$$

where $X_{i,p}$ is the number of times an amino acid i is found at position p, N is the number of different amino acids included in the random regions of the library ($N = 20$ for the library in this work), and $S_{i,p}$ is the score of amino acid i at position p. Once each amino acid had a score for each position in the peptide sequence, a SMALI score (S_m) was calculated for each peptide sequence by the summation of $S_{i,p}$ values for all randomized positions (from position −4 to 0). A peptide with a higher SMALI score has a stronger propensity to bind the query PDZ domain.

Synthetic Peptides. All peptides were synthesized and purified by GenScript Inc. (Piscataway, NJ). The peptides used were >95% pure as judged by analytical HPLC and mass spectrometry. Peptides for fluorescence anisotropy-based binding assays were dansylated at their N-termini. The concentration of peptide in solution was determined by measuring the UV absorbance at 280 nm using the extinction coefficient of the danysl-peptide calculated from the peptide sequence (SEDNTERP version 1.09)

and the dansyl group (*32*). The following peptides were used in this study: library-derived Tiam-binding peptides ($YAAKAFRF_{COOH}$, $YAAYRYRA_{COOH}$, $YAAGRKHF_{COOH}$, $YAALIHKF_{COOH}$, $YAAEKYWA_{COOH}$, $YAARKFAK_{COOH}$, $YAAKRTYV_{COOH}$, and $YAAQKHFH_{COOH}$), Model ($SSRKEYYA_{COOH}$) (*25*), human Syndecan1 (residues 303−310, $TKQEEFYA_{COOH}$), human Caspr4 (residues 1301−1308, $ENQKEYFF_{COOH}$), Caspr4(F→A) ($ENQKEYFA_{COOH}$), Syndecan1(A→F) ($TKQEEFYF_{COOH}$), and human Neurexin1 (residues 1470−1477, $NKDKEYYV_{COOH}$).

Equilibrium Fluorescence Binding Assay. Fluorescence anisotropy was used to monitor the binding of dansylated peptides to the Tiam1 and Tiam2 PDZ domains. The PDZ domain protein (1.5 mM stock) was titrated into a solution containing 1.3 mL of 1 μM dansylated peptide until little or no change in the measured anisotropy was evident. Fluorescence anisotropy measurements were recorded in a quartz cuvette at 25 °C with constant stirring using a Fluorolog-3 (Horiba Jobin Yvon) or LS-55 (Perkin-Elmer) spectrofluorometer. The excitation and emission wavelengths were set to 340 and 550 nm, respectively. The excitation and emission slit widths were adjusted to 3 nm (excitation) and 8 nm (emission), respectively, and individual measurements were integrated over 3 s. The data were baseline corrected using a buffer blank, and the titration curves were fit to a standard hyperbolic binding model (eq 1):

$$A - A_{min} = \frac{B_{max}[PDZ]}{K_d + [PDZ]} \quad (1)$$

where A is the anisotropy at each titration step, A_{min} is the initial anisotropy, B_{max} is the maximal anisotropy at PDZ domain saturation, K_d is the dissociation constant, and [PDZ] is the total concentration of the PDZ domain in solution. B_{max} and K_d were determined by fitting the titration data to eq 1 using nonlinear regression analysis (SigmaPlot, Systat Software Inc.). For presentation (see Figure 3), data were normalized to the fitted B_{max}. The reported dissociation constants are the average of at least three independent experiments. Using this assay, reliable quantification of the dissociation constant for PDZ domain−model peptide interactions was possible to approximately 250 μM.

The change in the Gibbs free energy of the PDZ domain−ligand interaction was determined by eq 2:

$$\Delta G_b = RT \ln(K_d) \quad (2)$$

where R is the gas constant, T is 298.15 K, and K_d is the fitted dissociation constant. The standard error in ΔG_b was propagated by standard methods (*33*). The coupling free energy was determined by eq 3:

$$\Delta\Delta G_{int} = (\Delta G_{WT} - \Delta G_{M1}) - (\Delta G_{M2} - \Delta G_{DM}) \quad (3)$$

where ΔG_{WT} is the free energy of peptide binding for the wild-type Tiam1 PDZ domain, ΔG_{DM} is the free energy of binding for the PDZ domain double mutant, and ΔG_{M1} and ΔG_{M2} are the binding energies for the respective PDZ domain single mutants.

RESULTS

We and others have previously reported on the specificity and protein binding partners of the Tiam1 PDZ domain (*8*, *25*, *26*). However, less is known about the specificity of the Tiam2 PDZ domain, and questions remain about its specificity for peptide ligands. Here, we investigated differences in the specificities of the Tiam1 and Tiam2 PDZ domains and determined the thermodynamic origin of these differences.

Determination of Tiam1 and Tiam2 PDZ Domain Specificities by Screening a Peptide Library. We have previously synthesized a one-bead-one-compound (OBOC) peptide library with a free C-terminus on 90 μm TentaGel resin (*29*). In this library, each bead is topologically segregated into two layers. The surface layer displays an inverted peptide with variable sequence and a free C-terminus of the form resin-$MLLBBEAAX^{-4}X^{-3}X^{-2}X^{-1}X^{0}_{COOH}$, where B is β-alanine and X^{-4}−X^{0} represent L-α-aminobutyrate (Abu or C, a replacement of cysteine), L-norleucine (Nle or M, a replacement of methionine), or any of the remaining 18 amino acids (Figure 2). The interior layer of the bead contains the corresponding peptide in the normal orientation (with a free N-terminus), which serves as an encoding tag for determining the sequence of the peptide. The library has a theoretical diversity of 20^5 or 3.2×10^6. We conducted library screening by incubating the OBOC library (typically 10−50 mg of the library resin) with fluorescently labeled or biotinylated GST−PDZ domain fusion protein and selecting those beads that were fluorescent or turquoise-colored (using an on-bead streptavidin−alkaline phosphatase and BCIP substrate) (*29*). The stringency of the screening was controlled (by varying the amount of GST−PDZ domain fusion protein and staining reaction time) so that ~0.05% of the library beads (typically 10−60 beads) became positive. The resulting positive beads, which should carry peptides of the highest affinities to the target protein, were manually removed from the library and individually sequenced by PED−MS (*30*). Note that macromolecules such as the GST−PDZ domain fusion proteins are too large to diffuse into the TentaGel beads and therefore only accessible to the inverted peptides on the bead surface. Thus, the encoding peptides in the bead interior do not interfere with library screening.

The Tiam1 PDZ domain was screened against a total of 102 mg of the library (~290000 beads) in six separate experiments to give a total of 126 positive beads. Although the number of beads and/or peptides screened represented only ~10% of the library sequence space, we have previously shown that the consensus sequence(s) of a typical protein domain can be unambiguously determined by screening only 10% of the library, because not all of the random positions are required for binding to the target proteins (*29*, *34*). Sequencing of the 126 beads by PED−MS (*30*) gave 106 reliable sequences (Table 1); for the other 20 beads, the quality of their mass spectra was too poor to allow for definitive sequence assignment. All six screening experiments gave the same types of (though not identical) sequences, demonstrating the reproducibility of the screening procedure. The 106 sequences were initially sorted into four different groups on the basis of sequence similarities with the aid of Microsoft Excel. Subsequently, each group of sequences was treated with SMALI (*31*) analysis to construct a

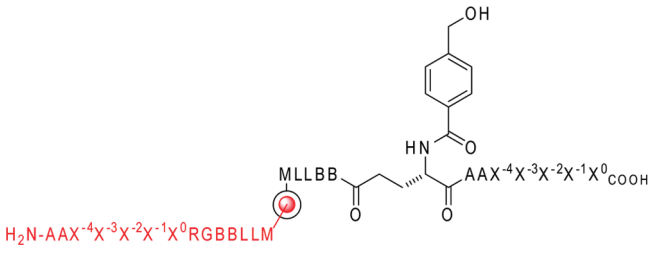

FIGURE 2: Scheme showing the structure of the inverted peptide library. B, β-alanine.

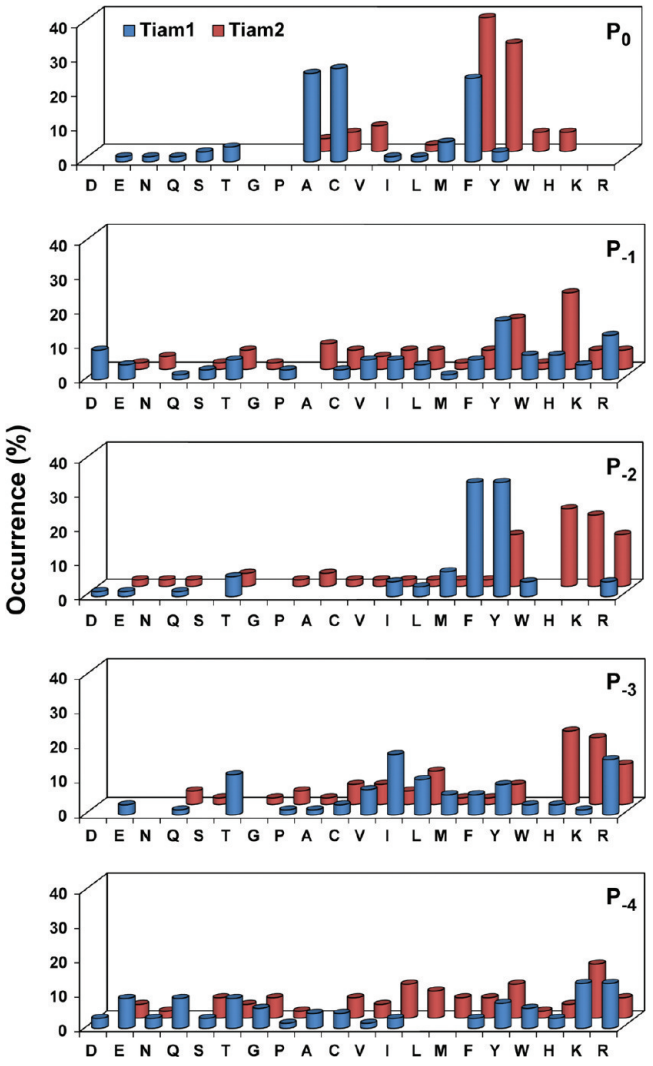

FIGURE 3: Sequence specificity of Tiam1 and Tiam2 PDZ domains. The histograms indicate the amino acids identified in the combinatorial peptide screen. Each position in the peptide is labeled P_0−P_{-4} starting from the C-terminus. The "Occurrence (%)" on the *y*-axis represents the percentage of the selected sequences (groups I and II) that contained a particular amino acid at a given position. C, (*S*)-2-aminobutyric acid (Abu); M, norleucine (Nle).

position-weighted matrix and assign a SMALI score (S_m), which indicates the propensity of the peptide to bind to the query PDZ domain (Table 1). The group I ligands have a consensus sequence of X-Φ-[F/Y]-X-$[A/Abu]_{COOH}$ (where Φ is a hydrophobic residue, especially β-branched amino acids, while X is any amino acid) (Table 1 and Figure 3). The 10 sequences that do not contain Ala or Abu at position P_0 all have very low SMALI scores (<1), suggesting that are either weak binders or false positives. The group II ligands (23 sequences) have a similar preference for a Phe/Tyr at P_{-2} and predominantly contain Phe at position P_0, which is occasionally replaced with Nle or Tyr. Interestingly, the group II ligands show a significant preference for a positively charged residue (Arg or Lys) at position P_{-4}, a trend not observed for the group I ligands (Table 1). The group III peptides are rich in basic residues (Arg and Lys) at all positions, whereas the group IV peptides each contain an H-X-H or H-X-X-H motif. We have observed both group III and IV sequences during our studies with other PDZ and SH2 domains and found that they have no measurable affinity for the protein domains used in the

Table 1: Peptide Library Sequences Selected by the GST−Tiam1 PDZ Domain Fusion Protein (total of 106)[a]

group I (47)				group II (23)		group III (23)	group IV (13)
peptide	S_m	peptide	S_m	peptide	S_m	peptide	peptide
RTYYC	1.88	VTFTA	1.49	KRFTF	4.29	FPRVR	PLHCH
ATYYC	1.87	EVFIC	1.49	RRFHF	4.23	YRYQR	YSHLH
IIYDC	1.86	HTFMA	1.48	RLFRF	4.15	FSDWK	ACHSH
GIYYA	1.85	RVFLA	1.45	KFFRF	4.10	XXXRR	HKHPY
QIYDA	1.84	QHFSA	1.40	KAFRF[b]	4.10	FTKRR	FTHKH
HTYRC	1.84	GILYC	1.26	KEFFF	4.02	CRFRK	CHLHV
NIYFC	1.82	YIIHC	1.25	TVFPF	3.72	RKFRR	HPHCR
AIYHA	1.80	YLIDC	1.18	ELYYF	3.37	KRFPR	HIHNC
NVYYC	1.79	RLRYC	1.16	CRYRF	3.37	KYRVR	HEHLG
TMYRC	1.78	WTWEC	1.16	KYTYF	3.27	RKFKR	HQHMR
ITYKA	1.77	WFIDA	1.10	EIYIF	3.20	RKFAK[b]	RHSLH
YRYRA[b]	1.75	KMMFC	1.10	YRRYF	3.12	XXGFK	HRVGH
YYYKC	1.74	SYWIA	1.03	PIYVF	3.07	GTKWR	RHLQH
TMYLA	1.71	KYYWS	0.94	EHMHF	3.03	XARTR	
RWYTA	1.66	WRFVT	0.75	DLMFF	3.02	RRSRV	
EKYWA[b]	1.66	FRTWT	0.40	TRWQF	3.01	YYKRD	
DFYCA	1.66	EMMLT	0.35	XXX YF	2.62	KRWTE	
AEYVA	1.65	QVTPN	0.30	RIFTM	2.22	RYKYN	
KIFRC	1.60	GLRII	0.27	WRFEM	2.13	RRVIT	
QIFDA	1.58	CWLKS	0.26	RQFYY	1.96	RRKYW	
SRFYC	1.54	GPTHQ	0.25	FCFEM	1.86	KRRHY	
TRFRC	1.54	CLDWE	0.22	KYMDM	1.45	KRKTY	
TTFCA	1.51	QCESL	0.18	RYQWY	0.91	LRKRY	
QFFVC	1.49						

[a]Underlined sequences were selected by the SA-AP/BCIP method, whereas the rest of the sequences were selected against Texas Red-labeled GST−PDZ domain fusion protein. M, norleucine; C, (*S*)-2-aminobutyric acid; X, amino acid identity could not be determined; S_m, SMALI score. [b]Sequences selected for further binding analysis.

screens (*29*, *35*). Two of the group III ($YAARKFAK_{COOH}$) and group IV peptides ($YAAQKHFH_{COOH}$) were synthesized with dansyl chloride at the N-terminus and tested for binding to Tiam1 and Tiam2 PDZ domains in the solution phase. Both peptides failed to bind to any of the PDZ domains (vide infra). The group III sequences are likely caused by the high ligand density on TentaGel beads (~100 mM), which permits a negatively charged protein molecule (or a negatively charged surface patch) to electrostatically interact with multiple peptides on the bead surface (*35*). The origin of the group IV peptides, which are primarily associated with the SA-AP/BCIP screening method, remains unknown. Thus, we consider both group III and IV sequences as false positives, although we cannot rule out the possibility that some of them may bind weakly to the Tiam1 PDZ domain, as our previous work has shown that certain weak ligands can be selected from a library if their specific binding (desired) is enhanced by undesired multidentate interactions (*35*).

Screening against the PDZ domain of Tiam2 yielded the same four groups of sequences (Table 2). The group I peptides that bind this PDZ domain are similar to those of the Tiam1 PDZ domain, except that Val was also selected at the C-terminus. The group II peptides were also similar to the group II peptides of the Tiam1 PDZ domain, in that they both selected an aromatic residue (Phe or Tyr) at the C-terminal position. However, the two PDZ domains show some key differences in their specificities. First, the Tiam1 PDZ domain selected predominantly Phe at position P_0, whereas the Tiam2 PDZ domain appears to bind Phe and Tyr equally well (Figure 3). Second, while the Tiam1 PDZ domain selected more group I peptides (47 sequences) than group II peptides (23 sequences), the Tiam2 PDZ domain selected a

much greater number of group II peptides (10:44 group I:group II ratio), suggesting that it has higher affinity for the group II sequences. Additionally, the group II peptides selected by the Tiam2 PDZ domain exhibited broader specificity at the C-terminal position, accepting bulkier side chains (e.g., Val) (Tables 1 and 2). Third, the Tiam1 PDZ domain strongly prefers Phe or Tyr at position P_{-2}, whereas the Tiam2 PDZ domain accepts both Tyr and positively charged residues (His, Lys, and Arg) (Figure 3). Overall, the results from the peptide library screen suggest that the Tiam1 and Tiam2 PDZ domains have overlapping but distinct specificities for peptide ligands and indicate that positions P_0 and P_{-2} are the most crucial determinants for their specificities. The group III and IV sequences are deemed false positives. The Tiam2 PDZ domain selected a smaller number of false positive sequences as compared to the Tiam1 PDZ domain. This is likely due to the fact that the Tiam2 PDZ domain generally has higher affinities for the library peptides (vide infra) and is therefore less susceptible to interference from nonspecific binding (*34*).

Table 2: Peptide Library Sequences Selected by the GST−Tiam2 PDZ Domain Fusion Protein (total of 69)[a]

group I (10)		group II (44)				group III (3)	group IV (12)
peptide	S_m	peptide	S_m	peptide	S_m	peptide	peptide
FKYCC	3.32	CHKHF	2.04	GYHRY	1.53	TTSKR	YKHAH
IKYFA	3.24	GRKHF[b]	1.96	KYELF	1.53	DKQYR	QKHFH[b]
LKYFA	3.24	SLKHF	1.93	HCKRY	1.52	YMRRR	RRHFH
SKFYV	3.04	RHHCF	1.88	MHRAY	1.52		MRHFH
YHYAV	3.01	IHKSF	1.87	VKNFF	1.48		CRHIH
XKYYL	3.01	KYHVF	1.81	IKRIY	1.46		IYHKH
YHRHV	2.15	SRHAF	1.81	ERAHY	1.43		KSHRH
KRTYV[b]	2.10	LQKYF	1.80	XXYWF	1.42		EKHTH
WPMGC	1.51	KFHLF	1.79	GMRYY	1.41		IRHVH
MLHMC	1.51	FRHVF	1.79	NKRCY	1.41		CHLHR
		KHCHF	1.79	CHYRY	1.41		RHSHR
		KHPHF	1.79	XXXIF	1.37		HFHKR
		YSKYF	1.78	RLTEY	1.22		
		IIHTF	1.78	RQINY	1.20		
		LIHKF[b]	1.77	TGLLY	1.19		
		HPHKF	1.74	MRHNW	0.67		
		ILKHY	1.71	KLRYH	0.64		
		TKHHY	1.70	CVRYW	0.57		
		YKAHF	1.70	EVYAH	0.41		
		VCKHY	1.66	LVQIW	0.36		
		FCKHY	1.66	PAVTH	0.30		
		YHKKY	1.65				
		KHRTY	1.57				

[a]Underlined sequences were selected against Texas Red-labeled GST−PDZ domain fusion protein, whereas the rest of the sequences were selected by the SA-AP/BCIP method, followed by a secondary screen for Texas Red. M, norleucine; C, (*S*)-2-aminobutyric acid; X, amino acid identity could not be determined; S_m, SMALI score. [b]Sequences selected for further binding analysis.

Binding Affinities of Tiam1 and Tiam2 PDZ Domains for Peptide Ligands. To validate the library screening results, we randomly selected and synthesized three representative peptides for each PDZ domain ($YAAKAFRF_{COOH}$, $YAAYRYRA_{COOH}$, and $YAAEKYWA_{COOH}$ for Tiam1 and $YAAGRKHF_{COOH}$, $YAALIHKF_{COOH}$, and $YAAKRTYV_{COOH}$ for Tiam2) and determined their binding affinities by a fluorescence anisotropy assay. These peptides represent group I and II peptides that make up the major binding motif found in the library screen. As mentioned above, two group III and IV peptides were also tested and did not bind to either the Tiam1 or Tiam2 PDZ domain. In contrast, the three group I and II peptides tested for the Tiam2 PDZ domain bound with affinities typical for PDZ domains (K_d = 10−80 μM) and showed no detectable binding to the Tiam1 PDZ domain (Table 3). Interestingly, the three library-derived Tiam1 peptides only weakly bound the Tiam1 PDZ domain (K_d values from 90 to >250 μM) but bound the Tiam2 domain with higher affinities ($K_d \sim 20$ μM). The weak affinity of the Tiam1 PDZ domain also explains why library screening against this domain was more problematic and resulted in a larger number of false positive beads as compared to the number for the Tiam2 PDZ domain (Tables 1 and 2). A possible explanation for the generally weak binding of the Tiam1 PDZ domain is that residue P_{-5} may also contribute to binding (*8*). To test this notion, we synthesized and tested a peptide containing a Gln at position P_{-5}, because several Tiam1-interacting proteins contain a Gln at this position (Table 3). However, the

Table 3: Dissociation Constants (K_d) for the Interactions of the Tiam1 and Tiam2 PDZ Domains with Library and Physiological Peptides

		K_d (μM)	
Peptide	Sequence	Tiam1 PDZ	Tiam2 PDZ
Tiam1 peptide 1 (Group I)	YAA**YRYRA**	NB[a]	22.5 ± 1.1
Tiam1 peptide 2 (Group I)	YAA**EKYWA**	90.3 ± 8.3	10.9 ± 0.4
Tiam1 peptide 3 (Group II)	YAA**KAFRF**	200 ± 50	7.7 ± 1.3
Tiam1 peptide 4 (Group III)	YAA**RKFAK**	NB[a]	NB[a]
Tiam2 peptide 1 (Group I)	YAA**KRTYV**	NB[a]	77.6 ± 2.4
Tiam2 peptide 2 (Group II)	YAA**GRKHF**	NB[a]	9.9 ± 2.2
Tiam2 peptide 3 (Group II)	YAA**LIHKF**	NB[a]	28.7 ± 4.9
Tiam2 peptide 4 (Group IV)	YAA**QKHFH**	NB[a]	NB[a]
		K_d (μM)	
Peptide	Sequence	Tiam1 PDZ	Tiam2 PDZ
Model	SSR**KEYYA**	112 ± 15[b,c]	24.1 ± 7.1
Syndecan1	TKQ**EEFYA**	26.9 ± 0.9[b]	200 ± 20
Syndecan1 (A→F)	TKQ**EEFYF**	55.7 ± 3.6[b]	4.5 ± 0.2
Caspr4	ENQ**KEYFF**	19.0 ± 0.4	3.4 ± 0.3
Caspr4 (F→A)	ENQ**KEYFA**	64.8 ± 5.9[b]	78.7 ± 7.8
Neurexin1	NKD**KEYYV**	2400 ± 250[b,c]	5.0 ± 0.2

[a]No binding detected within the limitations of the fluorescence binding assay (>250 μM). [b]Data taken from ref *8*. [c]Affinity based on NMR titration.

Table 4: Comparison of the Derived Consensus Sequences[a] for Tiam1 and Tiam2 PDZ Domain Ligands

	P_{-4}	P_{-3}	P_{-2}	P_{-1}	P_0
Tiam1 (*25*)	[X]	[I]	[FY]	[YH]	[AF]
Tiam1 (*26*)	[F]	[ILM]	[G]	[W]	[F]
Tiam1 (this study)[b]	[RK]	[IR]	[FY]	[YR]	[ACF]
Tiam2(*26*)	[R]	[STE]	[ST]	[SR]	[V]
Tiam2 (this study)[b]	[K]	[RKH]	[YRKH]	[YH]	[FY]

[a]Abbreviations: C, (*S*)-2-aminobutyric acid; X, any amino acid. [b]The indicated amino acids had an occurrence of 10% at each position, one standard deviation from the average.

addition of a Gln at position P_{-5} did not enhance binding, suggesting that this position does not significantly contribute to binding. Despite the fact that the selected library sequences had only weak affinity for the Tiam1 PDZ domain, the obtained preferences at each position closely recapitulate the consensus sequences identified by the previous studies of Songyang et al. (*25*) and Tonikian et al. (*26*), further validating the results of our screening. The derived consensus sequences for the Tiam1 and Tiam2 PDZ domains are listed in Table 4.

Potential Tiam1- and Tiam2-Binding Proteins. Using a composite consensus sequence based on the studies presented here and previous studies (*8*, *25*−*27*), we searched the PROSITE database (*36*) for candidate Tiam1 and Tiam2 PDZ domain-binding proteins. This analysis yielded 12 human proteins for Tiam1 and 43 proteins for Tiam2 (Tables S1 and S2 of the Supporting Information). Among the identified candidate proteins were Syndecan proteins, Contactin-associated protein-like 4 (Caspr4), and Neurexin1. Syndecans are cell−cell and cell−matrix adhesion proteins (*37*, *38*), and Caspr4 (*39*) and Neurexin1 (*40*, *41*) are neuronal cell−cell adhesion proteins of the Neurexin family. The four isoforms of Syndecan (1−4) have very similar C-terminal sequences, with the last four residues being $EFYA_{COOH}$; the four C-terminal residues of Caspr4 are $EYFF_{COOH}$, and Neurexin1 has a C-terminus of $EYYV_{COOH}$. The putative Tiam1 PDZ domain-binding proteins were consistent with those found previously (*8*), while those for the Tiam2 PDZ domain constitute a novel set of proteins that may link Tiam2 to new functions (Table S2 of the Supporting Information).

We next tested the two PDZ domains against peptide ligands derived from the C-termini of known and putative PDZ domain-binding proteins. We have previously shown that the C-terminal peptides from Syndecan1 ($TKQEEFYA_{COOH}$) and Caspr4 ($ENQKEYFF_{COOH}$) bound the Tiam1 PDZ domain with typical PDZ domain ligand affinities, whereas the Neurexin1 peptide ($NKDKEYYV_{COOH}$) bound with a very low affinity (Table 3) (*8*). Because the library screening indicated differences in specificity between the Tiam1 and Tiam2 PDZ domains, we investigated whether the Tiam2 PDZ domain could bind these physiologically relevant peptide ligands. The Caspr4 peptide matches both the Tiam1 and Tiam2 PDZ domain consensus sequences, and it indeed bound the Tiam2 PDZ domain with a K_d value of 3.4 μM, ~6-fold lower than that of the Tiam1 PDZ domain (Table 3). The Syndecan1 peptide, which does not match the Tiam2 consensus sequence, bound only very weakly to the Tiam2 PDZ domain (K_d ~ 200 μM). Given the general trend that the Tiam2 PDZ domain binds ligands with higher affinity than the Tiam1 PDZ domain, the weak binding of the Tiam2 PDZ domain for the Syndecan1 peptide suggests that this interaction is clearly not favored. In contrast, the Tiam2 PDZ domain bound the Neurexin1 peptide with high affinity (K_d = 5.0 μM), even though it contains a Val at the C-terminus, which was less frequently selected by the Tiam2 PDZ domain during library screening (Figure 3). This observation highlights the importance of acquiring individual binding sequences during library screening, as minor consensus sequences of this type (which bind to the target protein with high affinity but have low abundance in the library) would have been overlooked by some of the other library methods that select for both affinity and abundance [e.g., the oriented peptide library method (*25*)].

We previously employed Caspr4 and Syndecan1 peptides with point mutations at P_0 to examine the specificity of the Tiam1 PDZ domain (*8*). Here, we used these peptides to further probe the specificity of the Tiam2 PDZ domain at position P_0. Specifically, the C-terminal residues of the Syndecan1 and Caspr4 ligand were switched to Phe and Ala, respectively [denoted as Syndecan1-(A→F) and Caspr4(F→A), respectively]. We found that substitution of Ala for the C-terminal Phe of the Caspr4 peptide reduced its binding affinity for the Tiam2 PDZ domain by 23-fold, whereas replacement of the C-terminal Ala of the Syndecan1 peptide with a Phe increased the affinity by 44-fold (Table 3). These experiments corroborate the findings obtained from the peptide library screen and indicate that position P_0 is a key determinant that defines the specificity difference between the Tiam1 and Tiam2 PDZ domains and that a lack of optimal residues in P_0 seems to be partially offset in Tiam2 by the presence of a Tyr at position P_{-2}.

S_0 and S_{-2} Residues Selectively Modulate Ligand Affinity and Specificity. To establish the thermodynamic origin of the distinct specificity between the two Tiam PDZ domains, we probed the individual specificity pockets identified in the Tiam1 PDZ domain structure. To understand the roles of residues L915, L920, L911, and K912 in Tiam1 PDZ domain affinity and specificity, we created single-site mutants at each of these positions, changing the residue to the corresponding amino acid found in the Tiam2 PDZ domain. In addition, the double mutants L915F/L920V and L911M/K912E were created. For each mutant, the K_d and free energy of binding (ΔG_b, eq 2) were determined for the interaction with the Syndecan1 and Caspr4 peptides (Table 5). Syndecan1 binding was disrupted by all of the mutations in the S_0 pocket: the K_d was 3-fold higher in the case of L915F, 2-fold higher for L920V, and ~5-fold higher for the L915F/L920V double mutant. The Caspr4 binding data were more heterogeneous, with a ~3-fold increase in K_d for the L915F mutant, a ~2-fold decrease in K_d for the L920V mutant, and a 4-fold increase in K_d for the L915F/L920V double mutant. Binding of Neurexin1 to each single mutant was too weak to allow for reliable measurement of the K_d changes and was therefore not analyzed in detail. Notably, however, the L915F/L920V double mutant bound the Neurexin1 peptide with a K_d ~14-fold lower than that of the wild-type Tiam1 PDZ domain.

When residues in the S_{-2} pocket were probed, the L911M mutation did not disrupt binding to either the Syndecan1 or Caspr4 peptide, as both interactions had affinities similar to that of the wild-type Tiam1 PDZ domain (Table 5). The K912E mutation disrupted binding to both the Syndecan1 (5-fold) and Caspr4 (3-fold) peptides. Both the L911M and K912E mutants bound very weakly to the Neurexin1 peptide and were not analyzed further. The L911M/K912E double mutant, however, exhibited significant impairment in Syndecan1 binding (~8-fold), yet its affinity for the Caspr4 peptide was nearly the same as that for the wild-type Tiam1 PDZ domain. Finally, the Neurexin1 peptide bound to the L911M/K912E double mutant with a K_d ~9-fold lower than that for the wild-type Tiam1 PDZ domain.

Table 5: Pairwise Coupling Free Energies of Interaction ($\Delta\Delta\Delta G_{int}$) for Tiam1 PDZ Domain Mutants as a Function of Binding the Syndecan1, Caspr4, and Neurexin1 Peptide Ligands[a]

Tiam1 PDZ domain	K_d (μM)	ΔG_b[b]	$\Delta\Delta G_b$[c]	$\Delta\Delta\Delta G_{int}$[d]	$\sum$singles
		Syndecan1 ($TKQEEFYA_{COOH}$)			
wild type	26.9 ± 0.90	-6.23 ± 0.02			
L911M	34.7 ± 0.70	-6.08 ± 0.01	0.15 ± 0.02		
K912E	140 ± 20	-5.25 ± 0.08	0.98 ± 0.09		
L911M/K912E	211 ± 36	-5.00 ± 0.10	1.20 ± 0.10	0.07 ± 0.13	1.13 ± 0.09
L915F	81 ± 7	-5.58 ± 0.05	0.65 ± 0.06		
L920V	46 ± 3	-5.92 ± 0.03	0.31 ± 0.04		
L915F/L920V	250 ± 20	-4.91 ± 0.08	1.32 ± 0.09	0.36 ± 0.13	0.96 ± 0.07
QM	122 ± 8	-5.33 ± 0.04	0.89 ± 0.04		
		Caspr4 ($ENQKEYFF_{COOH}$)			
wild type	19.0 ± 0.40	-6.43 ± 0.01			
L911M	14.0 ± 0.30	-6.61 ± 0.01	-0.18 ± 0.02		
K912E	58.6 ± 4.10	-5.77 ± 0.04	0.67 ± 0.04		
L911M/K912E	28.9 ± 0.90	-6.19 ± 0.02	0.24 ± 0.02	-0.25 ± 0.04	0.49 ± 0.04
L915F	61 ± 4	-5.74 ± 0.04	0.69 ± 0.04		
L920V	10.8 ± 0.60	-6.77 ± 0.03	-0.33 ± 0.04		
L915F/L920V	76.5 ± 3.4	-5.61 ± 0.04	0.75 ± 0.05	0.38 ± 0.10	0.36 ± 0.06
QM	18.3 ± 0.30	-6.46 ± 0.01	-0.02 ± 0.02		
		Neurexin1 ($NKDKEYYV_{COOH}$)			
wild type	2400 ± 250[e]	-3.60 ± 0.10			
L911M/K912E	270 ± 150	-4.90 ± 0.30	-1.30 ± 0.30		
L915F/L920V	166 ± 12	-5.15 ± 0.07	-1.58 ± 0.10		
QM	46 ± 2	-5.91 ± 0.04	-2.30 ± 0.10		

[a]Abbreviations: b, binding; int, interaction; QM, quadruple mutant (L911M/K912E/L915F/L920V). [b]Units of kilocalories per mole. [c]$\Delta\Delta G_b = \Delta G_b$(mutant) $- \Delta G_b$(wild-type). [d]$\Delta\Delta\Delta G_{int} = \Delta G_b$(mutant1,2) $- [\Delta G_b$(mutant1) $+ \Delta G_b$(mutant2)]. [e]Data taken from ref *8*.

These results suggest that residues in the S_0 and S_{-2} pockets are important for determining the specificity of the Tiam1 PDZ domain, and that their relative importance is dependent upon the peptide ligand being examined.

Double-Mutant Cycle Analysis of the S_0 and S_{-2} Binding Pocket Residues. We used double-mutant cycle analysis to further characterize the energy of interaction between sites mutated in the Tiam1 PDZ domain. This type of analysis involves construction of thermodynamic cycles from two mutants made individually and then together within the same protein, and measurement of free energy to determine whether these individual mutations cause additive changes in energetics (*42*). The results of the double-mutant cycle analysis are listed in Table 5. The two amino acids of the S_0 binding pocket that were probed (L915 and L920) were found to act cooperatively with respect to both Syndecan1 ($\Delta\Delta\Delta G_{int}$ = 0.36 kcal/mol) and Caspr4 ($\Delta\Delta\Delta G_{int}$ = 0.38 kcal/mol) binding. In both cases, most of the loss of binding energy was attributable to the L915F mutant, and the L920V mutant was unable to rescue binding. Double-mutant cycle analysis was also applied to residues L911 and K912 of the S_{-2} pocket. These residues were not coupled with respect to Syndecan1 binding ($\Delta\Delta\Delta G_{int}$ = 0.07 kcal/mol) but did act cooperatively ($\Delta\Delta\Delta G_{int}$ = -0.25 kcal/mol) with respect to Caspr4 peptide binding. These data indicate that residues L915 and L920 in the S_0 pocket work cooperatively to provide selectivity for both ligands. In contrast, energetic coupling between residues L911 and K912 was ligand-dependent, suggesting that they interact in a distinct manner with different ligands.

Residues in S_0 and S_{-2} Pockets Determine Tiam1 and Tiam2 PDZ Domain Specificity. Having established that single and double Tiam1 PDZ domain mutations within the S_0 and S_{-2} binding pockets can modify ligand specificity, we next combined the four mutations in the binding pockets to produce a Tiam1 quadruple mutant (QM) and determined the combined effect on binding the Syndecan1, Caspr4, and Neurexin1 peptides. While none of the single or double mutants was able to fully re-create the specificity profiles of the Tiam2 PDZ domain, the quadruple mutant Tiam1 PDZ domain did; it was able to bind both the Caspr4 and Neurexin1 peptides but not the Syndecan1 peptide (Figure 4). The Tiam1 QM PDZ domain bound the Caspr4 peptide with approximately the same K_d as the wild-type PDZ domain, while the affinity for the Neurexin1 peptide was enhanced 52-fold. In contrast, the Tiam1 QM PDZ domain bound the Syndecan1 peptide with a 5-fold greater K_d than did the wild-type PDZ domain. Comparison of the Tiam1 QM PDZ domain with the Tiam2 PDZ domain indicated that although the peptide specificity profiles of the two are the same, their affinity for these peptides was distinct. For example, the QM PDZ domain bound the Caspr4 peptide with a 5-fold higher K_d, the Neurexin1 peptide with a 9-fold higher K_d, and the Syndecan1 peptide with a 1.6-fold lower K_d than did the Tiam2 PDZ domain. Taken together, these data show that the four mutations in the Tiam1 PDZ domain alone are sufficient to effectively recapitulate the binding specificity of the Tiam2 PDZ domain, but additional mutations are needed to match the affinities of the Tiam2 PDZ domain precisely.

DISCUSSION

The Tiam1 and Tiam2 GEF proteins have generally been assumed to have similar and overlapping functions within the cell (*43*, *44*). This notion is reinforced by the fact that both proteins have similar domain compositions and high degrees of

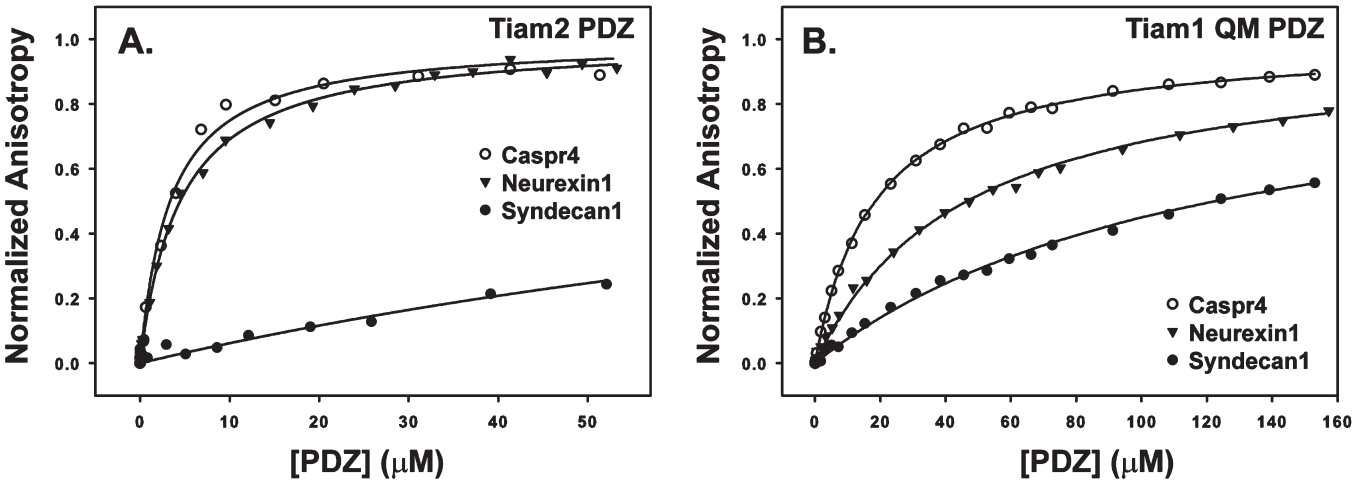

FIGURE 4: The Tiam1 PDZ domain quadruple mutant (QM) has the same specificity as the Tiam2 PDZ domain. Representative peptide binding curves for (A) the Tiam2 PDZ domain and (B) the Tiam1 PDZ domain QM (L911M, K912E, L915F, and L920V). Individual curves are for interactions with the (○) Caspr4, (▼) Neurexin1, and (●) Syndecan1 peptides. Each titration curve was measured in triplicate.

sequence conservation in the PH_n-CC-Ex and DH-PH_c catalytic domains (Figure 1A). Furthermore, the PH_n-CC-Ex domains of both proteins show redundancy in structure and binding partners (*45*), and both DH-PH_c domains are known to specifically activate the Rac1 GTPase (*21*). Nevertheless, close examination of other domains in Tiam1 and Tiam2 proteins, such as the PDZ domain, suggests that this functional redundancy may not apply to all domains. Previous studies on the specificity of the Tiam1 and Tiam2 PDZ domains have generated significant discrepancies. We sought to resolve these discrepancies by using a novel combinatorial peptide screen (*29*) to independently determine the consensus binding sequences for the Tiam1 and Tiam2 PDZ domains. Furthermore, we were interested in determining the molecular origin of the Tiam family PDZ domain specificity.

Rationalizing Tiam1 and Tiam2 PDZ Domain Specificities. The study by Songyang et al. (*25*) showed that the Tiam1 PDZ domain has a preference for peptides containing Phe or Ala at the C-terminal position (P_0) (Table 4). Tonikian et al. (*26*) reported that the Tiam1 PDZ domain preferred Phe at P_0, but not Ala. Our results show that both Phe and Ala are preferred residues at position P_0. Additionally, our study reveals a preference for Abu, used as a cysteine replacement. The preference for Ala (or Abu) can be readily explained by the structure of the Tiam1 PDZ domain, which has a shallow S_0 pocket accepting the small methyl group of Ala, whereas a conformational change(s) in this pocket or the peptide ligand may be necessary to accommodate the larger side chain of Phe (*8*). Table 4 shows that the Tiam1 PDZ domain had amino acid preferences for N-terminal residues of the ligand as well. All previous studies indicate that the PDZ domain prefers a hydrophobic side chain (Tyr and Trp) at position P_{-1} (Table 4). Our results show that Arg is also preferred and almost all amino acids are tolerated. The Tiam1 PDZ domain−model peptide structure shows that the P_{-1} side chain points to the solvent, although it can make hydrophobic and/or hydrogen bonding interactions with residues S861, N876, and S877 in the S_{-1} pocket (*8*). At position P_{-2}, we found that the Tiam1 PDZ domain is highly selective for aromatic residues (Phe and Tyr), in agreement with the results of Songyang et al. (*25*). The Tiam1 PDZ domain−model peptide structure shows that the Tyr side chain fits snugly into a large, deep pocket on the PDZ domain surface (*8*). It is unclear why the phage display experiment of Tonikian et al. (*26*) selected Gly exclusively at this position. The Tiam1 PDZ domain again tolerates a variety of amino acids at position P_{-3} but has some preference for residues containing larger hydrophobic side chains (e.g., Ile, Tyr, Leu, and Arg) (Figure 3). In the PDZ domain−model peptide structure (Figure 1C), the P_{-3} side chain is exposed to the solvent and therefore many different residues are accommodated at this position. However, the β- and γ-methylene groups of the P_{-3} Glu are engaged in hydrophobic interactions with both the PDZ domain surface and the side chain of residue P_{-1} (Tyr), and this may provide some degree of selectivity. Finally, the Tiam1 PDZ domain has broad specificity with some preference for charged residues (Arg, Lys, and Glu) at position P_{-4}. The broad specificity is explained by the fact that the P_{-4} side chain is mostly exposed to the solvent in the Tiam1 PDZ domain−model peptide structure (Figure 1D). Thus, the particular preferences for ligand residues at positions P_0−P_{-4} by the Tiam1 PDZ domain are readily rationalized by the Tiam1 PDZ domain−model peptide structure.

Our results show that the Tiam2 PDZ domain has a distinct but overlapping specificity compared to that of the Tiam1 PDZ domain. A major distinction between these two PDZ domains is at position P_0. Although the two PDZ domains accept (and selected from the library) the same set of amino acids at position P_0 (Ala, Abu, Phe, and Tyr), they have very different relative preferences for these residues. The Tiam1 PDZ domain selected Ala and Phe with similar frequencies, and the actual binding affinity for each (Ala vs Phe) depends on the sequence context of positions P_{-5}−P_{-1}. The Tiam2 PDZ domain, on the other hand, clearly prefers Phe and Tyr over Ala (Figure 3 and Table 3). However, with optimal sequences at other positions, peptides with a C-terminal Ala and Val may still bind to the Tiam2 PDZ domain with respectable affinities (Table 3). In particular, the peptide from Neurexin1 (containing Val at the C-terminus) was in fact one of the most potent peptide ligands of the Tiam2 PDZ domain identified in this study (K_d = 5.0 μM). Thus, it appears that the work of Tonikian et al. (*26*) identified a minor consensus class of Tiam2 ligands. It is not yet clear why their method did not select the major consensus class of ligands, which are generally more potent ligands than those of the minor class.

The Tiam2 PDZ domain was also selective for residues P_{-4}−P_{-1} of the ligand. Similar to the Tiam1 PDZ domain, it prefers hydrophobic and positively charged residues at position

P_{-1}. A homology model of the Tiam2 PDZ domain based on the structure of the Taim1 PDZ domain suggests that the residues surrounding residue P_{-1} form a hydrophobic patch and that D845 in β3 of the Tiam2 PDZ domain (S877 in the Tiam1 PDZ domain) could form a salt bridge with surrounding basic side chains. Another major difference in specificity compared to the Tiam1 PDZ domain is at position P_{-2}. The Tiam2 PDZ domain strongly prefers Tyr and the positively charged His, Lys, or Arg at this position. The preference for positively charged amino acids at this position is likely due to the presence of a glutamic acid near the P_{-2} binding pocket in the Tiam2 PDZ domain (corresponding to residue K912 in the Tiam1 PDZ domain). The selection of charged residues at position P_{-4} might also be due to the Glu at position 912. Together, these results indicate that the Tiam1 and Taim2 PDZ domains have overlapping but distinct specificities, and that the P_0 and P_{-2} positions in the ligand are the major determinants of Tiam1 and Tiam2 PDZ domain specificity.

Origin of Tiam Family PDZ Domain Specificity. On the basis of the results from the peptide screen, structural data, and the primary sequence alignment of the Tiam1 and Tiam2 PDZ domains, we hypothesized that the differences in the specificities of these proteins are determined primarily by the residues at positions P_0 and P_{-2} of the ligand and residues in the S_0 and S_{-2} pockets of the PDZ domain that participate in protein−ligand interactions. Here we sought to identify the residues that determine the specificity of these two PDZ domains and to establish if we could rationally re-engineer PDZ domain specificity by making targeted mutations in the S_0 and S_{-2} pockets.

As described in our previous study, the S_0 binding pocket in the Tiam1 PDZ domain is shallow and formed in part by L915 in α2 and L920 found in strand β6 (Figure 1D). Notably, neither of these residues is conserved between the Tiam1 and Tiam2 PDZ domains (Figure 1B). On the basis of the Tiam1 PDZ domain−Model peptide structure (*8*), we hypothesized that substituting residues in this pocket with those found at these positions in Tiam2 might enable the Tiam1 PDZ domain to bind Tiam2 PDZ domain ligands. Our results with the S_0 pocket mutants showed that the L915F mutant disrupted Caspr4 peptide binding but that the L920V mutant exhibited enhanced binding. In addition, the S_0 pocket double mutant L915F/L920V disrupted Caspr4 binding (~4-fold) and Syndecan1 binding (~9-fold), revealing a modest negative cooperativity in both cases. These results suggest that L915 and L920 contribute to ligand specificity by selecting residues in P_0 and, in the case of the Tiam1 PDZ domain, are fine-tuned to accommodate Ala and Phe. In contrast, residues in the S_0 pocket of the Tiam2 PDZ domain prefer ligands with a C-terminal Phe/Tyr and Val over those that contain Ala at this position. While neither single S_0 mutant could accommodate a Val at the C-terminal position, the double mutant acquired the ability to bind the Neurexin1 peptide at the expense of its ability to bind the Syndecan1 peptide, arguing that these two residues synergistically contribute to Tiam1 PDZ domain specificity.

Examination of the structure of the Tiam1 PDZ domain−Model peptide structure indicates that residues L911 and K912 form a pocket that packs against the Tyr at position P_{-2} of the ligand (Figure 1C,D) (*8*). In addition, this structure shows that residue Lys P_{-4} of the Model ligand is ~7 Å from K912 of the PDZ domain. In the case of the Syndecan1 peptide, residue P_{-4} is a Glu, and one can imagine that a salt bridge might form between this side chain and that of K912. This hypothesis is supported by the binding results with the K912E mutant, which reduced the level of Syndecan1 peptide binding to the level seen with the Model peptide. The L911M mutant did not have a strong effect on the binding of either Syndecan1 or Caspr4 ligand, and this mutation was incapable of rescuing Syndecan1 ligand binding in the presence of K912E. In contrast, the L911M/K912E double mutant had a cooperative affect, restoring Caspr4 binding levels near that seen with the wild-type protein. Interestingly, this double mutant also exhibited a marked increase in affinity for Neurexin1. Together, these results show that the S_{-2} pocket has little influence on Caspr4 peptide specificity and affinity yet profoundly affects interactions with Syndecan1 and Neurexin1. Thus, it appears that PDZ domain−ligand interactions are optimized distinctly for each ligand.

A Quadruple Mutant Leads to the Switch in Specificity of the Tiam1 PDZ Domain. Each of the double mutants tested had vestigial Tiam2 PDZ domain specificity, such that Caspr4 peptide binding was mildly perturbed at the expense of Syndecan1 peptide binding and interactions with the Neurexin1 peptide were always enhanced. Remarkably, the four mutations were highly synergistic when combined. The Tiam1 QM PDZ domain bound the Caspr4 peptide with an affinity indistinguishable from that measured with the wild-type Tiam1 PDZ domain, while the Neurexin1 peptide bound with a K_d ~52-fold lower than that of the wild-type PDZ domain. In addition, the Tiam1 QM PDZ domain significantly disrupted the Syndecan1 peptide interaction. Thus, the four mutations found in the S_0 and S_{-2} pockets effectively switched the specificity of the Tiam1 PDZ domain to that of the Tiam2 PDZ domain. The structural origin of this change in specificity is not fully understood but likely reflects stabilizing interactions between the S_0 and S_{-2} pockets.

Cooperative Effects and Engineering PDZ Domain−Ligand Binding Interactions. Our results show that PDZ domain specificity can be rationally re-engineered via incorporation of only a few specific mutations. Thus, engineered Tiam family PDZ domains with particular specificities could be used to probe PDZ domain-dependent functions. In general, such switches have been difficult to achieve and have been possible only when elaborate biological screens or computational algorithms were implemented (*46*−*48*). The re-engineering process was simplified in this case by the fact that the Tiam1 and Tiam2 PDZ domains have overlapping specificity. In particular, the interaction between residue K912 and ligand residue P_{-4} appears to be important in establishing PDZ domain specificity playing a critical role in promoting Syndecan1 peptide binding. Our findings also revealed that specificity subsites in the Tiam1 PDZ domain are coupled and that this coupling is dependent upon the ligand. Although not tested here, cooperativity between subsites might also be important. The fact that mutations in the S_0 and S_{-2} pockets were synergistic in changing the Tiam1 PDZ domain specificity hints that these couplings might exist. Our results support the notion that PDZ domain affinity and specificity are regulated by determinants spread across the entire binding site rather than by a few discrete subsites (*8*, *27*, *49*, *50*). This feature would likely allow the broad range of PDZ domain specificities needed to accommodate interactions with many potential ligands but would also complicate the design of novel specificities. Thus, cooperative effects may present a significant challenge for designing de novo PDZ domain specificities when starting from a template backbone structure.

Evolutionarily Conserved Specificity of Tiam Family PDZ Domains. Having shown that four nonconserved residues are vital for determining the specificity of the Tiam1 PDZ domain, we examined if these residues might be evolutionarily conserved

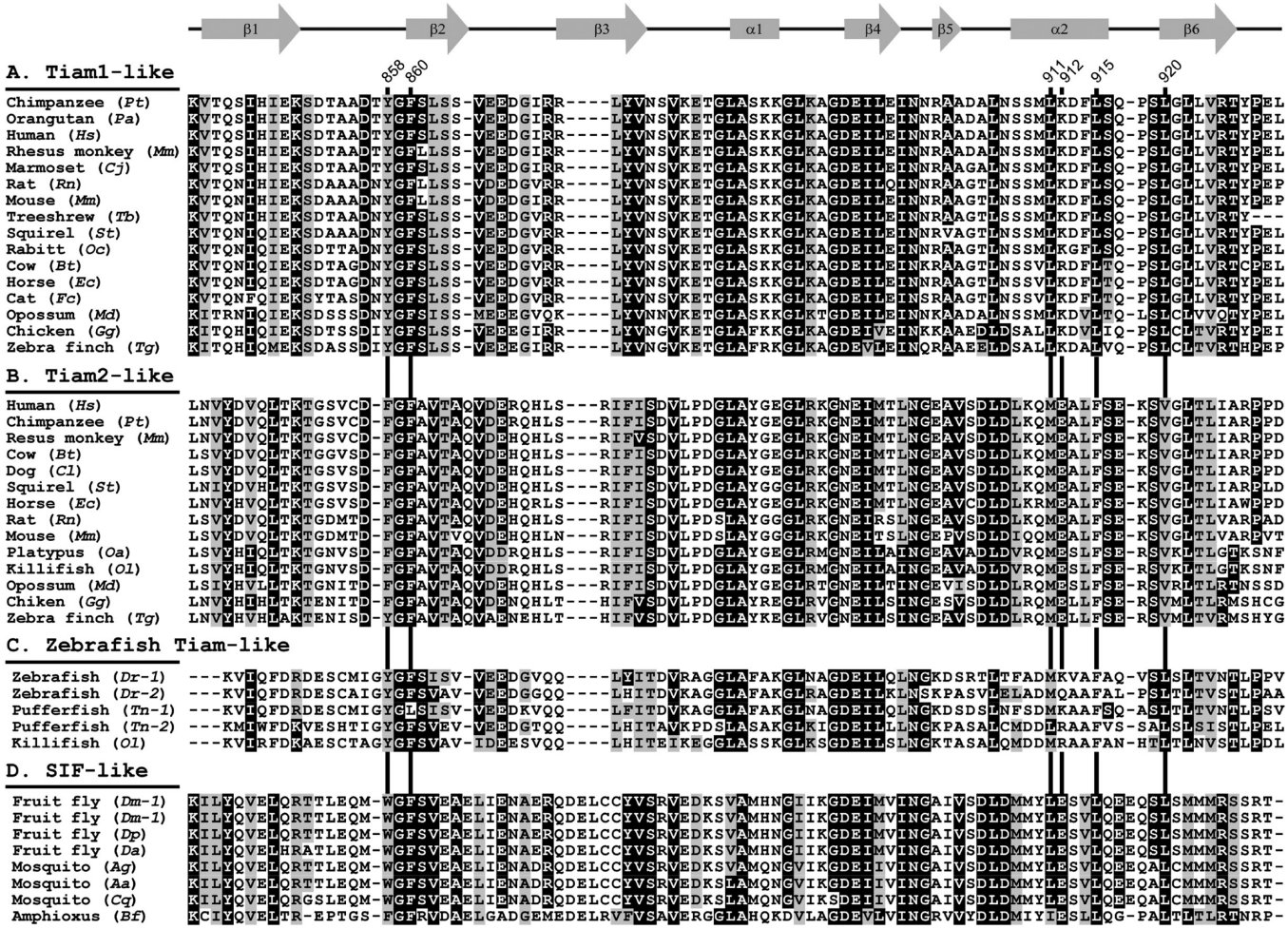

FIGURE 5: PDZ domains of Tiam family guanine exchange proteins can be classified into four subfamilies. Forty-three protein sequences were collected from the SMART database (*53*, *54*). The PDZ domain of each "Tiam-like" protein was aligned with the Tiam1 PDZ domain using ClustalX2 (*55*). The PDZ domains were grouped into four classes (A−D) based on the conservation of residues 911, 912, 915, and 920, respectively (numbered according to the Tiam1 PDZ domain). The protein accession numbers for these proteins are as follows: (A) Tiam1-like (*Pt*, UPI0000E25843; *Pa*, XP_002830672; *Hs*, Q13009-1; *Mm*, UPI0000D9A603; *Cj*, XP_002761403; *Rn*, UPI0000DA3756; *Mm*, Q60610; *Tb*, ENSTBEP00000012843; *St*, ENSSTOP00000005270; *Oc*, XP_002716851; *Bt*, UPI0000F33E72; *Ec*, UPI00015606CF; *Fc*, ENSFCAP00000002181; *Md*, ENSMODP00000037826; *Gg*, UPI0000ECD4E6; *Tg*, XP_002188532), (B) Tiam2-like (*Hs*, Q8IVF5; *Pt*, UPI0000E21226; *Mm*, UPI0000DC5170; *Bt*, UPI0000F3232D; *Cl*, UPI0000EB44DA; *St*, ENSSTOP00000000705; *Ec*, UPI00015607E2; *Rn*, UPI0000DC1DFF; *Mm*, UPI0000DC5170; *Oa*, ENSOANP00000010710; *Ol*, ENSOANP00000010712; *Md*, ENSMODP00000029251; *Gg*, UPI0000ECC8B0; *Tg*, XP_002198583), (C) zebrafish Tiam-like (*Dr-1*, XP_002664748; *Tn-1*, Q4RFR9; *Dr-2*, XP_001924044; *Tn-2*, Q4SFX7; *Ol*, ENSORLP00000005549), and (D) SIF-like (*Dm-1*, P91621; *Dm-2*, P91620; *Dp*, Q2LZN8; *Da*, B3M3N2; *Ag*, Q7PI66; *Aa*, Q17DC1; *Cq*, B0X8E7; *Bf*, C3YH98).

throughout the Tiam family of proteins. In addition, we were curious whether the PDZ domain could be used to effectively classify Tiam family GEFs, as shown by Sakarya et al. (*51*) for other PDZ domain-containing proteins. To this end, we compiled a collection of Tiam family PDZ domain sequences and aligned them on the basis of the known structure of the Tiam1 PDZ domain (Figure 5). Figure 5 clearly shows that the Tiam family PDZ domains segregate into four distinct families: Tiam1-like, Tiam2-like, zebrafish Tiam-like, and Drosophila Still Life (SIF, a GEF)-like (*52*). This analysis revealed that the four residues targeted in our study were differentially conserved across these four Tiam PDZ domain families, suggesting that PDZ domain specificities among members of this family are distinct across subfamilies but evolutionarily conserved within them. For example, the four residues investigated here are absolutely conserved within the vertebrate Tiam1 and Tiam2 PDZ domains. In the zebrafish Tiam-like and SIF-like counterparts, different sets of these four residues are conserved and the specificities of these hybrid PDZ domains remain unknown. Overall, these observations of PDZ domain conservation support the notion that Tiam family GEFs have divergent, PDZ domain-dependent functions that are evolutionarily conserved. Because only two in vivo PDZ domain-binding partners for Tiam1 have been identified (*8*, *24*) and none have been identified for either Tiam2 or SIF, additional studies will be required to experimentally assess the function of the Tiam2 and hybrid PDZ domains.

Implications for PDZ Domain-Dependent Tiam Family Protein Function. Previously, we identified the cell adhesion proteins Syndecan1 and Caspr4 as putative as Tiam1-binding proteins. In the case of Syndecan1, we showed that it was indeed a physiological partner of Tiam1 involved in cell migration and cell−matrix adhesion (*8*). Furthermore, we showed that this interaction occurred via the PDZ domain of Tiam1 and the C-terminus of Syndecan1. Here, we have identified 43 putative Tiam2-binding proteins, including the neuronal adhesion proteins Neurexin1 and Caspr4 (Table S2 of the Supporting Information). The Tiam2 PDZ domain is capable of binding peptides from both Neurexin1 and Caspr4 (Table 3) but not

Syndecan1. In contrast, the Tiam1 PDZ domain is capable of binding a Syndecan1 and Caspr4 C-terminal peptide but not a Neurexin1 peptide. Combined, these results strongly suggest that the Tiam1 and Tiam2 PDZ domains target distinct proteins leading to divergent functions. Importantly, our results predict that Neurexin1 and Tiam2 are binding partners in vivo, while Tiam1 is not. It is interesting to note that Neurexins and Caspr4 primarily function within neuronal cells where Tiam2 is known to function. It remains to be seen if the cell−cell adhesion function ascribed to the Neurexin family of receptor proteins may be connected with Tiam2's role in neurite extension via a PDZ domain interaction. Additional biological studies will be required to verify these predictions.

Conclusions. In the study presented here, we investigated the origin of the specificities of the Tiam1 and Tiam2 PDZ domains. Using a combinatorial peptide library screen and PDZ domain ligands from native proteins, we determined that these two PDZ domains have overlapping but distinct specificities. This result is of particular interest because these two homologous proteins are thought to be functionally redundant in many contexts (*21*, *44*); the distinct PDZ domain specificities suggest they may instead have unique biological functions conferred by each PDZ domain. Another important feature of our study was the identification of four residues in two specificity pockets (S_0 and S_{-2}) in the Tiam1 PDZ domain that are crucial for ligand affinity and specificity. Remarkably, replacing these four residues with the corresponding amino acids in the Tiam2 PDZ domain was sufficient to switch the specificity of the Tiam1 PDZ domain to that of the Tiam2 PDZ domain. Additionally, we found that residues in the S_0 and S_{-2} pockets were energetically coupled, and that the degree of coupling was dependent upon the identity of the ligand. Together, these results suggest that the interactions between PDZ domains and their ligands are highly evolved, and that specificity is derived from determinants spread across the entire binding interface. Finally, inspection of available Tiam family PDZ domain sequences provided further evidence that the Tiam family PDZ domains have evolved distinct specificities that likely translate into distinct PDZ domain-dependent functions.

ACKNOWLEDGMENT

We thank members of the Fuentes laboratory and Dr. C. M. Blaumueller for helpful discussions and comments on the manuscript and Dr. M. Hoshino (Kyoto University, Kyoto, Japan) for providing the full-length mouse Tiam2 DNA.

SUPPORTING INFORMATION AVAILABLE

Putative Tiam1 PDZ and Tiam2 PDZ binding proteins (Tables S1 and S2, respectively) and binding curves for various peptides identified in the combinatorial peptide screen (Figure S1). This material is available free of charge via the Internet at http://pubs.acs.org.

REFERENCES

1. Chiu, C. Y., Leng, S., Martin, K. A., Kim, E., Gorman, S., and Duhl, D. M. (1999) Cloning and characterization of T-cell lymphoma invasion and metastasis 2 (TIAM2), a novel guanine nucleotide exchange factor related to TIAM1. *Genomics 61*, 66–73.
2. Habets, G. G., van der Kammen, R. A., Stam, J. C., Michiels, F., and Collard, J. G. (1995) Sequence of the human invasion-inducing TIAM1 gene, its conservation in evolution and its expression in tumor cell lines of different tissue origin. *Oncogene 10*, 1371–1376.
3. Malliri, A., van Es, S., Huveneers, S., and Collard, J. G. (2004) The Rac exchange factor Tiam1 is required for the establishment and maintenance of cadherin-based adhesions. *J. Biol. Chem. 279*, 30092–30098.
4. Woodcock, S. A., Rooney, C., Liontos, M., Connolly, Y., Zoumpourlis, V., Whetton, A. D., Gorgoulis, V. G., and Malliri, A. (2009) SRC-induced disassembly of adherens junctions requires localized phosphorylation and degradation of the rac activator tiam1. *Mol. Cell 33*, 639–653.
5. Mertens, A. E., Rygiel, T. P., Olivo, C., van der Kammen, R., and Collard, J. G. (2005) The Rac activator Tiam1 controls tight junction biogenesis in keratinocytes through binding to and activation of the Par polarity complex. *J. Cell Biol. 170*, 1029–1037.
6. Nishimura, T., Yamaguchi, T., Kato, K., Yoshizawa, M., Nabeshima, Y., Ohno, S., Hoshino, M., and Kaibuchi, K. (2005) PAR-6-PAR-3 mediates Cdc42-induced Rac activation through the Rac GEFs STEF/Tiam1. *Nat. Cell Biol. 7*, 270–277.
7. Sander, E. E., van Delft, S., ten Klooster, J. P., Reid, T., van der Kammen, R. A., Michiels, F., and Collard, J. G. (1998) Matrix-dependent Tiam1/Rac signaling in epithelial cells promotes either cell-cell adhesion or cell migration and is regulated by phosphatidylinositol 3-kinase. *J. Cell Biol. 143*, 1385–1398.
8. Shepherd, T. R., Klaus, S. M., Liu, X., Ramaswamy, S., DeMali, K. A., and Fuentes, E. J. (2010) The Tiam1 PDZ domain couples to Syndecan1 and promotes cell-matrix adhesion. *J. Mol. Biol. 398*, 730–746.
9. Kunda, P., Paglini, G., Quiroga, S., Kosik, K., and Caceres, A. (2001) Evidence for the involvement of Tiam1 in axon formation. *J. Neurosci. 21*, 2361–2372.
10. Leeuwen, F. N., Kain, H. E., Kammen, R. A., Michiels, F., Kranenburg, O. W., and Collard, J. G. (1997) The guanine nucleotide exchange factor Tiam1 affects neuronal morphology; opposing roles for the small GTPases Rac and Rho. *J. Cell Biol. 139*, 797–807.
11. Tanaka, M., Ohashi, R., Nakamura, R., Shinmura, K., Kamo, T., Sakai, R., and Sugimura, H. (2004) Tiam1 mediates neurite outgrowth induced by ephrin-B1 and EphA2. *EMBO J. 23*, 1075–1088.
12. Tolias, K. F., Bikoff, J. B., Burette, A., Paradis, S., Harrar, D., Tavazoie, S., Weinberg, R. J., and Greenberg, M. E. (2005) The Rac1-GEF Tiam1 couples the NMDA receptor to the activity-dependent development of dendritic arbors and spines. *Neuron 45*, 525–538.
13. Tolias, K. F., Bikoff, J. B., Kane, C. G., Tolias, C. S., Hu, L., and Greenberg, M. E. (2007) The Rac1 guanine nucleotide exchange factor Tiam1 mediates EphB receptor-dependent dendritic spine development. *Proc. Natl. Acad. Sci. U.S.A. 104*, 7265–7270.
14. Hou, M., Tan, L., Wang, X., and Zhu, Y. S. (2004) Antisense Tiam1 down-regulates the invasiveness of 95D cells in vitro. *Acta Biochim. Biophys. Sin. 36*, 537–540.
15. Minard, M. E., Ellis, L. M., and Gallick, G. E. (2006) Tiam1 regulates cell adhesion, migration and apoptosis in colon tumor cells. *Clin. Exp. Metastasis 23*, 301–313.
16. Zhao, L., Liu, Y., Sun, X., He, M., and Ding, Y. (2010) Overexpression of T lymphoma invasion and metastasis 1 predict renal cell carcinoma metastasis and overall patient survival. *J. Cancer Res. Clin. Oncol.* (in press).
17. Engers, R., Mueller, M., Walter, A., Collard, J. G., Willers, R., and Gabbert, H. E. (2006) Prognostic relevance of Tiam1 protein expression in prostate carcinomas. *Br. J. Cancer 95*, 1081–1086.
18. Ding, Y., Chen, B., Wang, S., Zhao, L., Chen, J., Chen, L., and Luo, R. (2009) Overexpression of Tiam1 in hepatocellular carcinomas predicts poor prognosis of HCC patients. *Int. J. Cancer 124*, 653–658.
19. Rooney, C., White, G., Nazgiewicz, A., Woodcock, S. A., Anderson, K. I., Ballestrem, C., and Malliri, A. (2010) The Rac activator STEF (Tiam2) regulates cell migration by microtubule-mediated focal adhesion disassembly. *EMBO Rep. 11*, 292–298.
20. Yoshizawa, M., Hoshino, M., Sone, M., and Nabeshima, Y. (2002) Expression of stef, an activator of Rac1, correlates with the stages of neuronal morphological development in the mouse brain. *Mech. Dev. 113*, 65–68.
21. Matsuo, N., Hoshino, M., Yoshizawa, M., and Nabeshima, Y. (2002) Characterization of STEF, a guanine nucleotide exchange factor for Rac1, required for neurite growth. *J. Biol. Chem. 277*, 2860–2868.
22. Ponting, C. P. (1997) Evidence for PDZ domains in bacteria, yeast, and plants. *Protein Sci. 6*, 464–468.
23. Schultz, J., Copley, R. R., Doerks, T., Ponting, C. P., and Bork, P. (2000) SMART: A web-based tool for the study of genetically mobile domains. *Nucleic Acids Res. 28*, 231–234.
24. Masuda, M., Maruyama, T., Ohta, T., Ito, A., Hayashi, T., Tsukasaki, K., Kamihira, S., Yamaoka, S., Hoshino, H., Yoshida, T., Watanabe, T., Stanbridge, E. J., and Murakami, Y. (2010) CADM1 interacts with Tiam1 and promotes invasive phenotype of human T-cell leukemia virus

type I-transformed cells and adult T-cell leukemia cells. *J. Biol. Chem. 285*, 15511–15522.
25. Songyang, Z., Fanning, A. S., Fu, C., Xu, J., Marfatia, S. M., Chishti, A. H., Crompton, A., Chan, A. C., Anderson, J. M., and Cantley, L. C. (1997) Recognition of unique carboxyl-terminal motifs by distinct PDZ domains. *Science 275*, 73–77.
26. Tonikian, R., Zhang, Y., Sazinsky, S. L., Currell, B., Yeh, J. H., Reva, B., Held, H. A., Appleton, B. A., Evangelista, M., Wu, Y., Xin, X., Chan, A. C., Seshagiri, S., Lasky, L. A., Sander, C., Boone, C., Bader, G. D., and Sidhu, S. S. (2008) A specificity map for the PDZ domain family. *PLoS Biol. 6*, e239.
27. Stiffler, M. A., Chen, J. R., Grantcharova, V. P., Lei, Y., Fuchs, D., Allen, J. E., Zaslavskaia, L. A., and MacBeath, G. (2007) PDZ domain binding selectivity is optimized across the mouse proteome. *Science 317*, 364–369.
28. Hoshino, M., Sone, M., Fukata, M., Kuroda, S., Kaibuchi, K., Nabeshima, Y., and Hama, C. (1999) Identification of the stef gene that encodes a novel guanine nucleotide exchange factor specific for Rac1. *J. Biol. Chem. 274*, 17837–17844.
29. Joo, S. H., and Pei, D. (2008) Synthesis and screening of support-bound combinatorial peptide libraries with free C-termini: Determination of the sequence specificity of PDZ domains. *Biochemistry 47*, 3061–3072.
30. Thakkar, A., Wavreille, A. S., and Pei, D. (2006) Traceless capping agent for peptide sequencing by partial Edman degradation and mass spectrometry. *Anal. Chem. 78*, 5935–5939.
31. Li, L., Wu, C., Huang, H., Zhang, K., Gan, J., and Li, S. S. (2008) Prediction of phosphotyrosine signaling networks using a scoring matrix-assisted ligand identification approach. *Nucleic Acids Res. 36*, 3263–3273.
32. Du, H., Fu, R. A., Li, J., Corkan, A., and Lindsey, J. S. (1998) PhotochemCAD: A computer-aided design and research tool in photochemistry. *Photochem. Photobiol. 68*, 141–142.
33. Bevington, P. R., and Robinson, D. K. (2003) Data reduction and error analysis, 3rd ed., McGraw-Hill, New York.
34. Sweeney, M. C., Wavreille, A. S., Park, J., Butchar, J. P., Tridandapani, S., and Pei, D. (2005) Decoding protein-protein interactions through combinatorial chemistry: Sequence specificity of SHP-1, SHP-2, and SHIP SH2 domains. *Biochemistry 44*, 14932–14947.
35. Chen, X., Tan, P. H., Zhang, Y., and Pei, D. (2009) On-bead screening of combinatorial libraries: Reduction of nonspecific binding by decreasing surface ligand density. *J. Comb. Chem. 11*, 604–611.
36. de Castro, E., Sigrist, C. J., Gattiker, A., Bulliard, V., Langendijk-Genevaux, P. S., Gasteiger, E., Bairoch, A., and Hulo, N. (2006) ScanProsite: Detection of PROSITE signature matches and ProRule-associated functional and structural residues in proteins. *Nucleic Acids Res. 34*, W362–W365.
37. Beauvais, D. M., and Rapraeger, A. C. (2004) Syndecans in tumor cell adhesion and signaling. *Reprod. Biol. Endocrinol. 2*, 3.
38. Xian, X., Gopal, S., and Couchman, J. R. (2010) Syndecans as receptors and organizers of the extracellular matrix. *Cell Tissue Res. 339*, 31–46.
39. Spiegel, I., Salomon, D., Erne, B., Schaeren-Wiemers, N., and Peles, E. (2002) Caspr3 and caspr4, two novel members of the caspr family are expressed in the nervous system and interact with PDZ domains. *Mol. Cell. Neurosci. 20*, 283–297.
40. Craig, A. M., and Kang, Y. (2007) Neurexin-neuroligin signaling in synapse development. *Curr. Opin. Neurobiol. 17*, 43–52.
41. Lise, M. F., and El-Husseini, A. (2006) The neuroligin and neurexin families: From structure to function at the synapse. *Cell. Mol. Life Sci. 63*, 1833–1849.
42. Horovitz, A. (1996) Double-mutant cycles: A powerful tool for analyzing protein structure and function. *Folding Des. 1*, R121–R126.
43. Kawauchi, T., Chihama, K., Nabeshima, Y., and Hoshino, M. (2003) The in vivo roles of STEF/Tiam1, Rac1 and JNK in cortical neuronal migration. *EMBO J. 22*, 4190–4201.
44. Matsuo, N., Terao, M., Nabeshima, Y., and Hoshino, M. (2003) Roles of STEF/Tiam1, guanine nucleotide exchange factors for Rac1, in regulation of growth cone morphology. *Mol. Cell. Neurosci. 24*, 69–81.
45. Terawaki, S., Kitano, K., Mori, T., Zhai, Y., Higuchi, Y., Itoh, N., Watanabe, T., Kaibuchi, K., and Hakoshima, T. (2010) The PHCCEx domain of Tiam1/2 is a novel protein- and membrane-binding module. *EMBO J. 29*, 236–250.
46. Schneider, S., Buchert, M., Georgiev, O., Catimel, B., Halford, M., Stacker, S. A., Baechi, T., Moelling, K., and Hovens, C. M. (1999) Mutagenesis and selection of PDZ domains that bind new protein targets. *Nat. Biotechnol. 17*, 170–175.
47. Reina, J., Lacroix, E., Hobson, S. D., Fernandez-Ballester, G., Rybin, V., Schwab, M. S., Serrano, L., and Gonzalez, C. (2002) Computer-aided design of a PDZ domain to recognize new target sequences. *Nat. Struct. Biol. 9*, 621–627.
48. Wiedemann, U., Boisguerin, P., Leben, R., Leitner, D., Krause, G., Moelling, K., Volkmer-Engert, R., and Oschkinat, H. (2004) Quantification of PDZ domain specificity, prediction of ligand affinity and rational design of super-binding peptides. *J. Mol. Biol. 343*, 703–718.
49. Kurakin, A., Swistowski, A., Wu, S. C., and Bredesen, D. E. (2007) The PDZ domain as a complex adaptive system. *PLoS One 2*, e953.
50. Chen, J. R., Chang, B. H., Allen, J. E., Stiffler, M. A., and MacBeath, G. (2008) Predicting PDZ domain-peptide interactions from primary sequences. *Nat. Biotechnol. 26*, 1041–1045.
51. Sakarya, O., Conaco, C., Egecioglu, O., Solla, S. A., Oakley, T. H., and Kosik, K. S. (2010) Evolutionary expansion and specialization of the PDZ domains. *Mol. Biol. Evol. 27*, 1058–1069.
52. Sone, M. (1997) Still life, a protein in synaptic terminals of *Drosophila* homologous to GDP-GTP exchangers. *Science 275*, 1405.
53. Letunic, I., Doerks, T., and Bork, P. (2009) SMART 6: Recent updates and new developments. *Nucleic Acids Res. 37*, D229–D232.
54. Schultz, J., Milpetz, F., Bork, P., and Ponting, C. P. (1998) SMART, a simple modular architecture research tool: Identification of signaling domains. *Proc. Natl. Acad. Sci. U.S.A. 95*, 5857–5864.
55. Larkin, M. A., Blackshields, G., Brown, N. P., Chenna, R., McGettigan, P. A., McWilliam, H., Valentin, F., Wallace, I. M., Wilm, A., Lopez, R., Thompson, J. D., Gibson, T. J., and Higgins, D. G. (2007) Clustal W and Clustal X version 2.0. *Bioinformatics 23*, 2947–2948.